Mater. Res. Soc. Symp. Proc. Vol. 1210 © 2010 Materials Research Society 1210-Q05-02

Screen-Printed Al Back Contacts on Si Solar Cells: Issues and Some Solutions

Vishal Mehta,[1, 2] Bhushan Sopori,[1] Robert Reedy,[1] Bobby To,[1] Helio Moutinho,[1] and N.M. Ravindra[2]
[1] National Renewable Energy Laboratory, Golden, CO 80401, USA
[2] New Jersey Institute of Technology, Newark, NJ 07102, USA

ABSTRACT

This paper identifies some mechanisms that lead to problems in back Al contact formation. Major issues are related to a basic problem that the Al melt has a large surface tension and tries to ball up during the firing step. Other issues arise from dissolution of the Si-Al interface and entrapment of glass within the Si-Al alloy. Si diffusion into Al can be applied to control the melt, while cooling rate can help improve the structure of various regions of the back contact for a favorable series resistance. We also discuss a modified time-temperature profile that can lead to a deep and uniform back-surface field.

INTRODUCTION

The fire-through contact metallization technique (also known as co-firing) is widely used to fabricate metal contacts in commercial crystalline and multicrystalline silicon (c-Si) solar cells. Contact firing requires preparation of N^+/P wafers, which are then coated with about 750 Å of SiN:H by a plasma-enhanced chemical vapor deposition process. Next, screen-printed contacts consisting of gridded, Ag-based front contacts and continuous, Al-based back contacts are applied. The firing of both contacts is performed simultaneously, typically in a belt furnace using a profile that peaks at about 800°C. In this process, silver paste on the front side etches SiN:H, which reacts with Si and makes a near-ohmic contact with the N^+-Si layer, and hydrogen diffuses into the Si substrate and passivates defects and impurities. On the back side, Al alloys with silicon to produce a back contact with a P+ back-surface field (BSF).

Considerable amount of work has been done to determine various reactions that occur during a firing process. In particular, the Ag-Si contact formation and hydrogen diffusion have been studied in much detail. However, in spite of the fact that Al-Si reactions are well understood, the formation of a good back contact is difficult to achieve. A back contact must meet many requirements as discussed in the next section. All of them necessitate the formation of a strong alloy between Si and Al. However, strong alloying of the Si-Al contact is accompanied by many issues that continue to prevent high-efficiency solar cell fabrication. These issues include the following: (i) Molten Al do not stick uniformly to the silicon surface because of its high surface tension and tendency to ball up (Figure 1). This figure also shows another problem—discoloration—it is often observed after extended firing; (ii) Strong contact formation is often accompanied by a variety of problems such as increased shunting and formation of holes in the cell; (iii) Glass (which is necessary for improving the mechanical properties of the contact) can be trapped within Al particles, thus preventing them from reaching the Si surface and leading to high series resistance.

This paper explores issues related to strong alloying that is required for Al back-contact formation to achieve the highest cell efficiencies. We have studied the kinetics of Si-Al alloy formation/solidification and explored the possibility of controlling the Si-Al interaction through

diffusion of Si into Al, as proposed in a previous paper [1]. We have found that by controlling Si diffusion, the melt flow can be controlled to eliminate or minimize the alloying issues.

Figure 1. Schematic illustrating various issues involved in good back-contact formation.

MAJOR REQUIREMENTS OF A BACK ALUMINUM CONTACT

An Al back contact must fulfill many requirements, including: (a) Forming a deep uniform P^+ region (typically > 10 µm) to serve as an effective BSF for minority-carrier reflection; (b) Creating a low-resistance ohmic contact to achieve a high fill factor in the cell; (c) Producing a smooth, bump-free surface to facilitate reliable packaging; and (d) Producing an optically reflective Si-Al interface for effective light-trapping. Additionally, because certain impurities (e.g., Fe) can diffuse readily and be trapped at the liquid Al, this process is expected to getter impurities efficiently [2]. These requirements demand a strong (i.e., higher temperature and longer time) firing cycle. However, strong alloying causes problems as mentioned in the previous section. Several researchers have proposed empirical solutions to address these problems [3, 4]. For example, reference [3] suggests that a certain thickness of Al layer is required to produce a stable melt. We have proposed using Si diffusion to initiate a Si-Al melt at the Si-Al interface to promote adhesion between Si and the molten Al [1]. Details of Si diffusion in Al and its effects on the melt stability will be given in a forthcoming publication [5].

EXPERIMENTAL

In our previous work, we determined that the Al-Si contact formation was strongly influenced by Si diffusion [1]. Hence, our experiments were aimed at investigating the effects of Si diffusion, particularly in making uniform Al melts and BSFs. Figure 2 illustrates a typical firing profile that is used in our study. It includes a Si diffusion region produced by extended annealing at temperatures near 550°C. Other regions are typical of those that are used in conventional firing. Briefly, only the important features of various temperature ranges are described here. In the temperature range of 300°–400°C), the organic solvents and binders are removed. These are added to the pastes to improve rheology and aid transfer of the same from the screen onto the cells in the screen-printing step. The temperature range of 400°–600°C is normally important for the front contact. At these temperatures, the glass frit in the front Ag paste softens and the molten glass etches the SiN:H film. Ag particles sinter in the presence of glass. We have included an additional step at 550°C to inject Si interstitials for backside melt control. The optimum duration of the Si-injection anneal was found to be between 4 and 6 s. The ramp-up from about 600°C and the ramp-down from the peak temperature (800°C) have important effects both on the front and the back. The effect on the front contact is described in detail elsewhere [6]. On the back contact, the higher peak temperature leads to a larger melt and a higher concentration of Si in the melt. The size of the agglomerated Al particles increases with temperature and duration through sintering. This increase in size is accompanied by entrapment

of liquid glass. The influence of the peak temperature on the p+ concentration can be assessed from a relevant section of the phase diagram [7]. By examining at the Si-rich solidus region of the phase diagram, one can see that at a peak temperature of 800°C, the Si-Al melt will be doped with about 0.004% Al (~10^{18}).

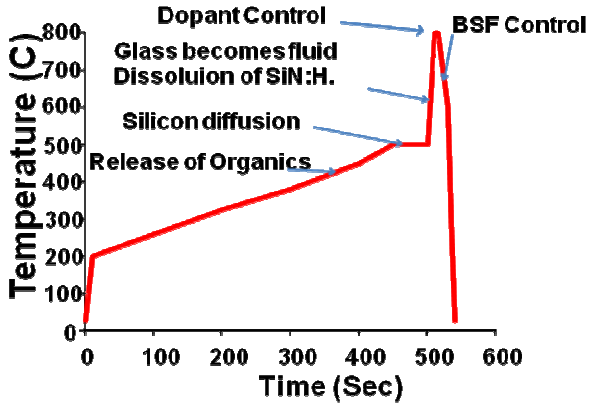

Figure 2. A time-temperature (t-T) firing profile showing functions of various regions.

Experiments were performed on two types of samples: (i) single-crystal, single-side polished Si wafers with evaporated Al layers of different thicknesses, and (ii) screen-printed, multicrystalline-Si (mc-Si) cells with and without front contacts. The samples were fired in a static optical furnace under various process conditions. Solar cells were characterized by current-voltage measurements and their cell parameters were determined. Cells were diced and large-area planar cross-sectioned (c/s) samples were prepared [8]. The fired samples were examined to determine structure, composition, and thickness of various layers. Optical microscopy of the c/s samples provided valuable information on melting of Al and formation of Si-Al alloy. Scanning electron microscopy (SEM) was used for high-resolution imaging of the processed contacts and for dopant profiling to study the BSF formation. Energy-dispersive X-ray (EDX) analysis was used for determining the composition of various alloyed regions. Scanning Kelvin probe microscopy (SKPM) was used to generate profiles to evaluate potential across the P+-P region and to determine local conductivity. Secondary-ion mass spectroscopy (SIMS) profiles were used to measure Si diffusion in Al and profiles of Al after firing. Some results of the results are presented here.

RESULTS

The structure of a typical contact formed by this process is shown in Figure 3. This figure is an optical micrograph of the cross-section showing the back contact of a cell, which involved Si diffusion for 6 s. The Si surface shows the texture and a Si-Al eutectic layer exists at the interface. The eutectic manifests itself as Si-rich and Al-rich phases. This can be observed at the valleys of the Si surface. Away from the interface, the aluminum particles are sintered and agglomerates of the enlarged particles are separated by inclusions of glass. The re-crystallized Al-doped Si side has retained some of the texture. Because this figure is an optical image, we do not see the BSF.

It is generally assumed that, during the firing process a melt is formed when the cell acquires the temperature of melting point of Al [9, 10]. However, as we have suggested before, Si can readily diffuse into Al with a high diffusivity at relatively low temperatures [11, 12].

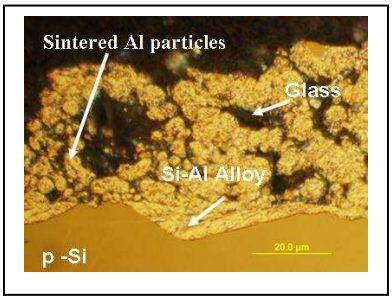

Figure 3. An optical micrograph of a c/s cell showing back Si-Al alloyed structure.

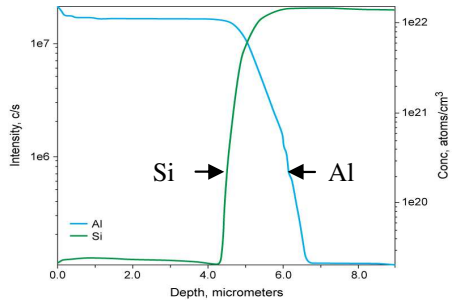

Figure 4. SIMS profiles of Si and Al for a sample processed at 550°C for 10 s.

Figure 4 shows SIMS profiles of Si and Al resulting from optical processing at 545°C for 10 s. The wafer was single-side polished, on which 4 µm of Al was deposited on the polished side. It can be seen that firing causes an intermixing of Si and Al, with a strong preferential diffusion of Si into Al. The diffusion of Si leads to a high concentration of Si at the interface and a buildup of Si interstitials in Al. We have found that Si diffusion stabilizes the Al melt. Under optimal conditions, the backside of the cell appears shiny-free from dimples, holes, and discoloration. We have examined the influence of including a Si injection step on the properties of the contact. Here, we specifically describe three aspects of the firing that are strongly influenced by Si diffusion: (1) influence of Si diffusion on the quality of the BSF, (2) influence of interface dissolution on texturing, and (3) influence of ramp-down rate on the structure of the back contact.

Influence of Si diffusion on the BSF

We have determined that a controlled silicon diffusion step results in a highly uniform BSF. Figure 5 shows an SEM micrograph taken in dopant contrast mode. As can be seen, the BSF is uniform and follows undulations of the interface. The Al-Si eutectic is seen to fill the texture valleys of the interface. It may be noted that while the thickness of the eutectic is changing, the BSF region is nearly constant. We have found that the maximum thickness of the BSF is controlled primarily by the thickness of Al. However, as discussed in the next section, the cooling rate has some influence.

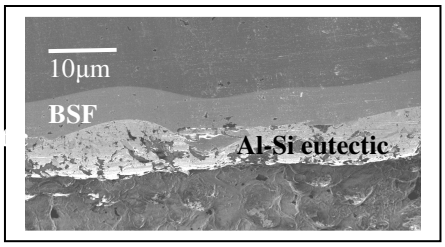

Figure 5. Dopant contrast SEM image of c/s cell showing a uniform BSF produced by Si injection alloying.

Effect on texturing and glass segregation

Because texturing exposes (111) planes, it produces various geometries for different grain orientations. Each of the interfaces experiences diffusion and dissolution during Si-Al alloy

formation. We performed experiments in which the melt is held for different durations, and we observed that, initially the melt fills the texture valleys and then spreads outward. Because of this, dissolution of the interface occurs preferentially at the sharp geometries. Figure 6b is a cross-section image of an alloyed sample showing rounding off of the sharp texture features. For comparison, we have also shown the corresponding front surface (Figure 6a) of the sample where no dissolution has occurred. The dissolution of the interface is expected to influence the light-trapping properties of the cell.

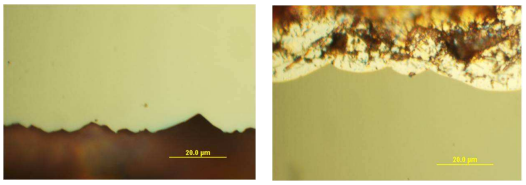

(a) (b)

Figure 6. C/s images showing the (a) front surface of cell, and (b) back interface.

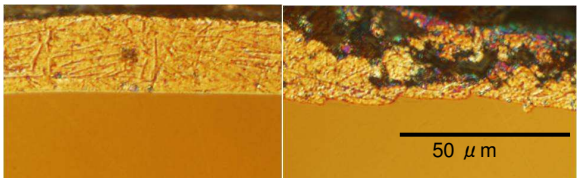

(a) (b)

Figure 7. C/s images of cells with (a) evaporated Al, and (b) screen-printed Al.

It is interesting to note that as the melt grows further, both glass and molten Si alloy have to coexist. However, on solidification, Si-Al alloy will freeze before the glass. Thus, patches of glass are trapped within the frozen Si-Al alloy. Figure 7b shows a typical cross-section of a screen-printed back side showing the presence of glass away from the Si interface. For comparison, we performed a similar process on a wafer with a thick layer of evaporated Al. Figure 7b is the corresponding cross-section of the alloyed, evaporated Al showing a continuous Si-Al alloy freeze out. The dispersion of glass within the Al back contact is expected to impede lateral flow of current and increase the series resistance (≈ 3%–4%) of the cell [13]. Figure 8a shows a schematic of the stratified back-contact layer. The collected carriers encounter glass and Si as they travel toward Ag/Pd pads. Another effect of glass entrapment is to prevent all of the aluminum to interact with Si. This leads to the formation of a non-uniform BSF.

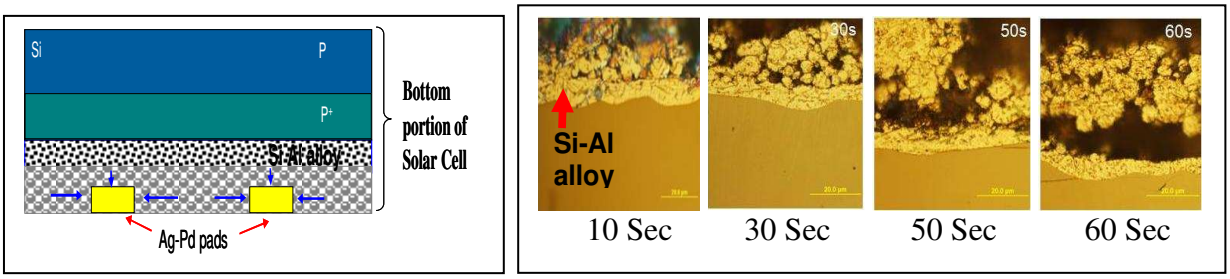

Figure 8. (a) Illustration of impedance to the current flow by trapped glass, and (b) cross-sections of various cells alloyed with different ramp-down times.

Ramp-down from peak temperature

During ramp down, the melt cools and tries to re-grow epitaxially over Si. This doped layer of Si follows the topology of the Si surface. On further cooling, the outside layer of Al freezes. This traps a liquid layer between solid Al (particles) and Si (with regions of soft glass). As the melt reaches the eutectic point, the entire melt is expected to freeze. It may be recognized that beyond the eutectic point, Si will continue to diffuse into Al-Si and will pile up at interstitial spaces. We performed experiments in which, time duration of cooling was varied arbitrarily from

800° to 577°C. As the cell cools from peak temperatures, the agglomerated mass of Al floats on the glass layer in some areas. As seen in Figure 8b, glass is trapped between sintered Al particles and Si-Al alloy for longer cooling times. This leads to the formation of a non-uniform BSF. Hence, longer cooling time (>15 s) from 800° to 577°C was not found to be beneficial.

CONCLUSIONS

We have found that many of the problems (i.e., Al spheres, holes, stains, and loss of light trapping) encountered in forming a good back contact can be mitigated by control of Si diffusion into Al, which occurs predominantly in the initial melting phase. Such defects are routinely seen during process optimization and can occur sporadically even in the well-optimized process in solar cell production. Si diffusion provides a source for forming a eutectic composition and is responsible for the initial melt formation at the eutectic point. A controlled eutectic interface enhances the adhesion of high-surface tension of molten Al and prevents Al from balling up. This mechanism also allows formation of a deep and uniform P+ layer during the solidification.

ACKNOWLEDGMENTS

This work was supported by the U.S. Department of Energy under Contract No. DOE-AC36-08GO28308 with the National Renewable Energy Laboratory.

REFERENCES

1. V. Mehta, B. Sopori, P. Rupnowski, H. Moutinho, A. Shaikh, C. Khadilkar, M. Bennett, and D. Carlson, *Mater. Res. Soc. Symp. Proc.* **1123,** Pittsburgh, PA, 2008, pp. 7–11.
2. P.S. Plekhanov, M.D. Negoita, and T.Y. Tan, *J. App. Phys.* **90**, 5388 (2001).
3. V. Meemongkolkiat, K. Nakayashiki, D.S. Kim, R. Kopecek, and A. Rohatgi, *J. Electrochem. Soc.* **153**, 1, G53 (2006).
4. F. Huster, *Proc. 20th European Photovoltaic Solar Energy Conference, Barcelona, 2005*, pp.1466–1469.
5. B. Sopori and V. Mehta, Back Al contact formation, to be published.
6. B. Sopori, V. Mehta, P. Rupnowski, D. Domine, M. Romero, H. Moutinho, B. To, R. Reedy, M. Al-Jassim, A. Shaikh, N. Merchant, and C. Khadilkar, *Proc. 22nd European Photovoltaic Solar Energy Conference, Milano, 2007*, pp. 841–848.
7. J.L. Murray and A.J. McAlister, *Bull. Alloy Phase Diagrams* **5**, 74 (1984).
8. B. Sopori, V. Mehta, N. Fast, H. Moutinho, D. Domine, B. To, and M. Al-Jassim, *Proc.17th Workshop on Crystalline Silicon Solar Cells & Modules: Materials and Processes, Vail, 2007*, pp. 222–227.
9. J.D. Alamo, J. Eguren, and A. Luque, *Solid-State Electron.* **24**, 415 (1981).
10. S. Narasimha, A. Rohatgi, and A.W. Weeber, *IEEE Trans. on Electron Devices* **46**, 7, 1999, pp. 1363–1369.
11. J.A. Amick, F.J. Bottari and J.I. Hanoka, *J. Electrochem. Soc.* **141**, 6, 1577 (1994).
12. J.O. McCaldin and H. Sankur, *Appl. Phys. Lett.* **19**, 12, 524 (1971).
13. B. Sopori, V. Mehta, D. Guhabiswas, R. Reedy, H. Moutinho, B. To, A. Shaikh, and A. Rangappan, *Proc 34th IEEE Photovoltaic Specialists Conference, Philadelphia, 2009*, pp.1963–1968.